

Simulations of the Domain State Model

U. Nowak¹, A. Misra², and K. D. Usadel¹

¹ Theoretische Physik, Gerhard-Mercator-Universität Duisburg
47048 Duisburg, Germany

² Dept. of Physics and MINT Center, University of Alabama
Box 870209, AL 35487, USA

ABSTRACT

The domain state model for exchange bias consists of a ferromagnetic layer exchange coupled to an antiferromagnetic layer. In order to model a certain degree of disorder within the bulk of the antiferromagnet, the latter is diluted throughout its volume. Extensive Monte Carlo simulations of the model were performed in the past. Exchange bias is observed as a result of a domain state in the antiferromagnetic layer which develops during the initial field cooling, carrying a remanent domains state magnetization which is partly irreversible during hysteresis. A variety of typical effects associated with exchange bias like, e. g. , its dependence on dilution, positive bias, temperature and time dependences as well as the dependence on the thickness of the antiferromagnetic layer can be explained within this model.

INTRODUCTION

For compound materials consisting of a ferromagnet (FM) in contact with an antiferromagnet (AFM) a shift of the hysteresis loop along the magnetic field axis can occur which is called exchange bias (EB). Often, this shift is observed after cooling the entire system in an external magnetic field below the Néel temperature T_N of the AFM. Although EB is well known since many years[1, 2] its microscopic origin is still discussed controversially. For a review of the vast literature on EB the reader is referred to an article by Nogués and Schuller [3].

In the approach of Malozemoff [4, 5, 6] EB is attributed to the formation of domain walls in the AFM, perpendicular to the FM/AFM interface due to interface roughness. These domain walls are supposed to occur during cooling in the presence of the magnetized FM and to carry a small net magnetization at the FM/AFM interface. This interface magnetization is furthermore supposed to be stable during the reversal of the FM, consequently shifting the hysteresis loop. However, the formation of domain walls in the AFM only due to interface roughness is energetically unfavorable and its occurrence and stability has never been proven.

Because of these difficulties other approaches have been developed. In a model introduced by Koon [7] EB is obtained through a mechanism in which a domain wall forms in the AFM parallel to the interface while the magnetization of the FM rotates. This mechanism has been proposed earlier by Mauri et al. [8]. Nevertheless it was shown by Schulthess and Butler [9, 10] that in this model EB vanishes if the motion of the spins in the AFM is not restricted to a plane parallel to the film as was done in Koon's work. To

obtain EB Schulthess and Butler assumed uncompensated AFM spins at the interface. However, their occurrence and stability during a magnetic hysteresis loop is not *explained*, neither in their model nor in other models [11, 12] although uncompensated AFM spins were observed experimentally [13, 14].

In a recent experiment Miltényi et al. [15] showed that it is possible to strongly influence EB in Co/CoO bilayers by diluting the antiferromagnetic CoO layer, i. e. by inserting non-magnetic substitutions ($\text{Co}_{1-x}\text{Mg}_x\text{O}$) or defects (Co_{1-y}O) not at the FM/AFM interface, but rather throughout the volume part of the AFM. In the same letter it was shown that a corresponding theoretical model, the domain state model, investigated by Monte Carlo simulations shows a behavior very similar to the experimental results. It was argued that EB has its origin in a domain state (DS) in the AFM which triggers the spin arrangement and the FM/AFM exchange interaction at the interface. Later it was shown that a variety of experimental facts associated with EB can be explained within this DS model [16, 17, 18, 19, 20].

The importance of defects for the EB effect is also confirmed by recent experiments on $\text{Fe}_x\text{Zn}_{1-x}\text{F}_2/\text{Co}$ bilayers [21] and by experiments [22, 23] where it was shown that it is possible to modify EB by means of irradiating an FeNi/FeMn system by He ions in presence of a magnetic field. Depending on the dose of the irradiation and the magnetic field present at the time of irradiation, it was possible to manipulate both the magnitude and even the direction of the EB field. Further support for the relevance of domains in EB systems is given by a direct spectroscopic observation of AFM domains [24, 25].

DOMAIN STATE MODEL

The domain state model [15] for EB consists of t_{FM} monolayers of FM and t_{AFM} monolayers of diluted AFM. The FM is exchange coupled to the topmost layer of the AFM. The geometry of the model is sketched in Fig. 1 for $t_{\text{FM}} = 1$ and $t_{\text{AFM}} = 3$.

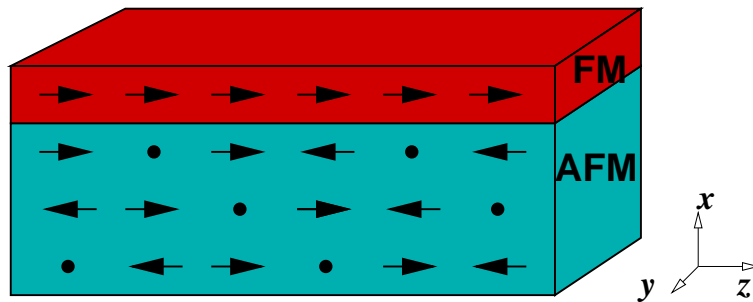


Figure 1: Sketch of the DS model with one FM layer and three diluted AFM layers. The dots mark defects. The easy axis of both, FM and AFM is the z - axis.

The system is described by a classical Heisenberg model with nearest neighbor exchange on a simple cubic lattice with exchange constants J_{FM} and J_{AFM} for the FM and the AFM respectively, while J_{INT} stands for the exchange constant between FM and AFM. For the nearest neighbor-exchange constant J_{AFM} of the AFM which mainly determines its

Néel temperature we set $J_{\text{AFM}} = -J_{\text{FM}}/2$. For simplicity, we assume the same value for the interface coupling, but with positive sign ($J_{\text{INT}} = -J_{\text{AFM}}$). Also, we assume that the values of the magnetic moments of FM and AFM are identical (included in the magnetic field energy B). The Hamiltonian of our system is thus,

$$\begin{aligned}
\mathcal{H} = & -J_{\text{FM}} \sum_{\langle i,j \rangle} \vec{S}_i \cdot \vec{S}_j - \sum_i \left(d_z S_{iz}^2 + d_x S_{ix}^2 + \vec{S}_i \cdot \vec{B} \right) \\
& -J_{\text{AFM}} \sum_{\langle i,j \rangle} \epsilon_i \epsilon_j \vec{\sigma}_i \cdot \vec{\sigma}_j - \sum_i \epsilon_i \left(k_z \sigma_{iz}^2 + \vec{\sigma}_i \cdot \vec{B} \right) \\
& -J_{\text{INT}} \sum_{\langle i,j \rangle} \epsilon_j \vec{S}_i \cdot \vec{\sigma}_j,
\end{aligned} \tag{1}$$

where \vec{S}_i denote normalized spins at sites of the FM layer and $\vec{\sigma}_i$ denote normalized spins at sites of the AFM.

The first line of the Hamiltonian describes the energy of the FM with the z -axis as its easy axis (anisotropy constant $d_z = 0.02J_{\text{FM}}$). d_z sets the Stoner-Wohlfarth limit of the coercive field, i. e., the zero temperature limit for magnetization reversal by coherent rotation ($B_c = 2d_z$, in our units, for a field parallel to the easy axis). The dipolar interaction is approximated by an additional anisotropy term (anisotropy constant $d_x = -0.1J_{\text{FM}}$) which includes the shape anisotropy, leading to a magnetization which is preferentially in the $y - z$ -plane. We checked, however, that its value does not influence our results, as far as the EB is concerned. The second line is the contribution from the AFM also having its easy axis along z direction. The AFM is diluted, i. e., a fraction p of sites is left without a magnetic moment ($\epsilon_i = 0$) while the other sites carry a moment ($\epsilon_i = 1$). The last term describes the interaction of the FM with the interface AFM monolayer.

Eq. 1 suggests a simple ground state argument for the strength of the bias field. Assuming that all spins in the FM remain parallel during field reversal and that some net magnetization of the interface layer of the AFM remains constant during the reversal of the FM a simple calculation gives the usual estimate for the bias field,

$$t_{\text{FM}} B_{\text{EB}} = J_{\text{INT}} m_{\text{INT}}, \tag{2}$$

where m_{INT} is that stable part of the interface magnetization of the AFM (per spin) which is responsible for the EB. For an ideal uncompensated and totally stable interface one would expect $m_{\text{INT}} = 1$. As is well known, this estimate leads to a much too high bias field, while for an ideal compensated interface, on the other hand, one would expect $m_{\text{INT}} = 0$ and, hence, $B_{\text{EB}} = 0$. Experimentally, however, often there is on the one hand no big difference between compensated and uncompensated interfaces and on the other hand it is found that B_{EB} is much smaller than $J_{\text{INT}}/t_{\text{FM}}$, rather of the order of a few percent of it. The solution of this puzzle is that m_{INT} is neither constant during field reversal nor is it a simple known quantity [19, 18] and we will discuss this in detail in the following.

RESULTS

Monte Carlo methods are used with a heat-bath algorithm and single-spin flip dynamics [26] for the simulation of the model explained above. The trial step of the spin update consists of two steps: first it is a small variation within a cone around the initial spin direction, followed, second, by a total spin flip. This twofold spin update is ergodic and symmetric [27] and can take care of a broad range of anisotropies, from very soft spins up to the high anisotropy (Ising) limit. We perform up to 40000 Monte Carlo steps (MCS) for a complete hysteresis loop.

To observe the domain structure of the AFM we have to guarantee that typical length scales of the domain structure fit into our system. In the following we show results for systems of lateral extension $L \times L$ with $L = 64$ or 128 and a thickness of $t_{\text{FM}} = 1$ and t_{AFM} ranging from 3 to 9. We use periodical boundary conditions within the film plane and open boundary conditions perpendicular to it.

The main quantities which we monitor are the thermal averages of the z -component of the magnetic moment for each individual monolayer normalized to the magnetic moment of the saturated monolayer. In our simulations the system is cooled from above to below the ordering temperature of the AFM. During cooling the FM is initially magnetized along the easy z axis resulting in a nearly constant exchange field for the AFM monolayer at the interface. Also, the system is cooled in the presence of an external magnetic field, the cooling field. In addition to the exchange field from the ordered FM this field acts also on the AFM. When the desired final temperature is reached a magnetic field along the easy axis is applied and reduced in small steps down to a certain minimum value and afterwards raised again up to the initial value. This corresponds to one cycle of the hysteresis loop.

Typical hysteresis loops are depicted in Fig. 2. Shown are results for the magnetization of the FM (upper figure) as well as that of the AFM interface monolayer (lower figure). An EB is observed clearly and we determine the corresponding EB field as $B_{\text{EB}} = (B^+ + B^-)/2$ where B^+ and B^- are those fields of the hysteresis loop branches for increasing and decreasing field, where the easy axis component of the magnetization of the FM becomes zero.

An analysis of the magnetization curve of the interface layer gives an interesting insight into the nature of EB. After the field cooling procedure the AFM interface carries a magnetization (m_{I}). A part of this AFM interface magnetization is stable during hysteresis and leads to the fact that the magnetization curve of the interface layer of the AFM is shifted upwards. This irreversible part of the interface magnetization of the AFM acts as an additional effective field on the FM, resulting in EB. Note that the interface magnetization of the AFM also displays hysteresis, following the exchange coupling to the FM. This means that the whole interface magnetization of the AFM consists of a reversible part leading to an enhanced coercivity and an irreversible part leading to EB.

In experiments usually the magnetization of the whole FM/AFM bilayer is measured. The corresponding sample magnetization loop might not only be shifted horizontally but also vertically. The vertical shift contains contributions from the volume part of the AFM as well as from its interface. The volume magnetization of the AFM is induced by the cooling field and hence not shifted when the cooling field is zero and shifted upwards when it is finite. The interface contribution depends on the sign of the interface coupling and

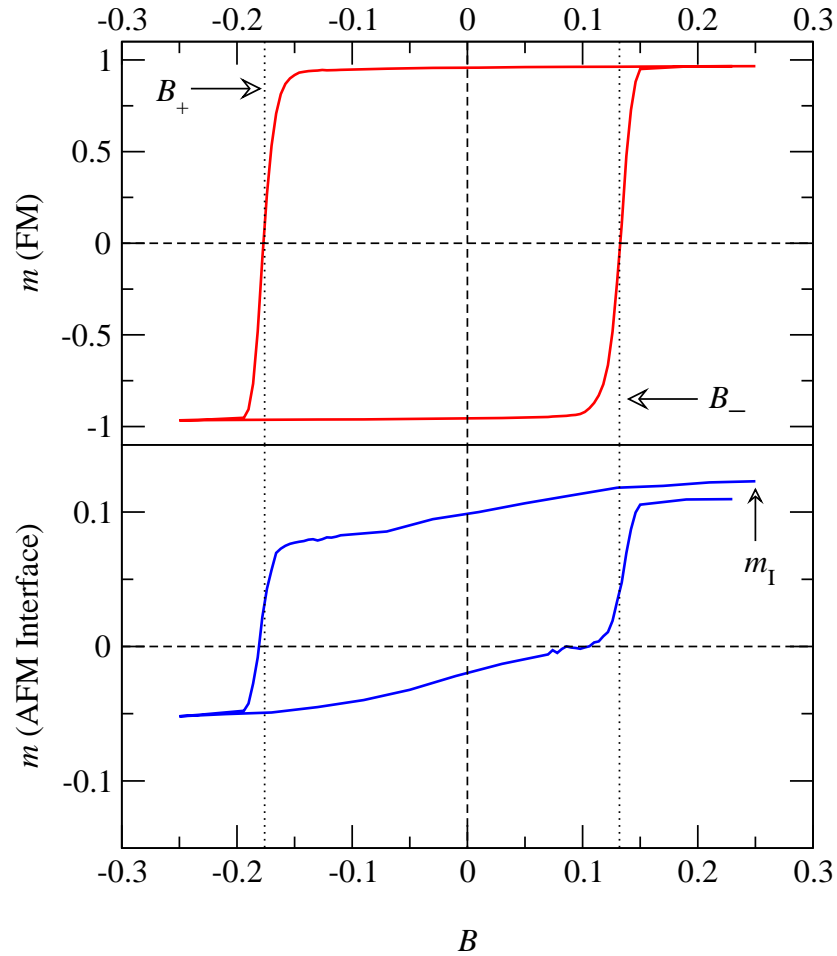


Figure 2: Simulated hysteresis loops of the DS model as explained in the text. Dilution $p = 0.4$, $k_B T = 0.1 J_{\text{FM}}$, positive interface coupling, $J_{\text{INT}} = |J_{\text{AFM}}|$. AFM anisotropy $k_z = J_{\text{FM}}/2$. The cooling field was $B_c = 0.25 J_{\text{INT}}$. Shown is the magnetic moment of the FM and the interface monolayer of the AFM (normalized to its saturation value.)

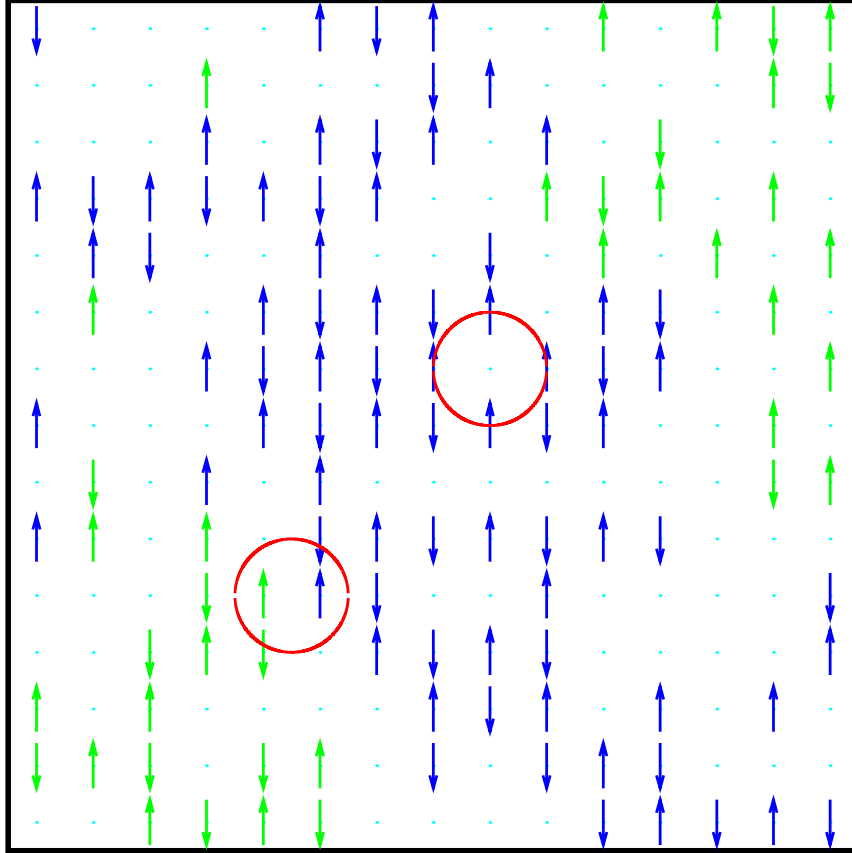


Figure 3: Snapshot of a spin configuration in a small portion of the interface monolayer of the AFM after field cooling ($B_c = 0.25J_{\text{FM}}$). The color coding distinguishes different AFM domains. The circles mark sources of magnetization. The external field and the FM magnetization are pointing up.

may be positive, as in our calculation, or even negative for negative interface coupling (see also [28, 19, 18]).

With the following two sketches we want to illustrate on a more microscopic basis where the interface magnetization of the AFM and its partitioning in reversible and irreversible parts comes from. Figure 3 shows spin configurations in a small portion of the interface monolayer of the AFM after field cooling. The simulated system size is $64 \times 64 \times 10$ with only one FM monolayer. For simplicity, this simulation was performed in the Ising limit for the AFM ($k_z \rightarrow \infty$). The dilution p of the AFM is 50 %, nevertheless the spins are much more connected than it appears from the sketch via the third dimension.

Obviously, the AFM is in a domain state. The reason for the domain formation and, consequently, for the lack of long-range order is the interface magnetization which couples to the exchange field coming from the FM and the external field (both pointing up) lowering the energy of the system. The interface magnetization follows from two contributions. Examples for both are indicated via the circles.

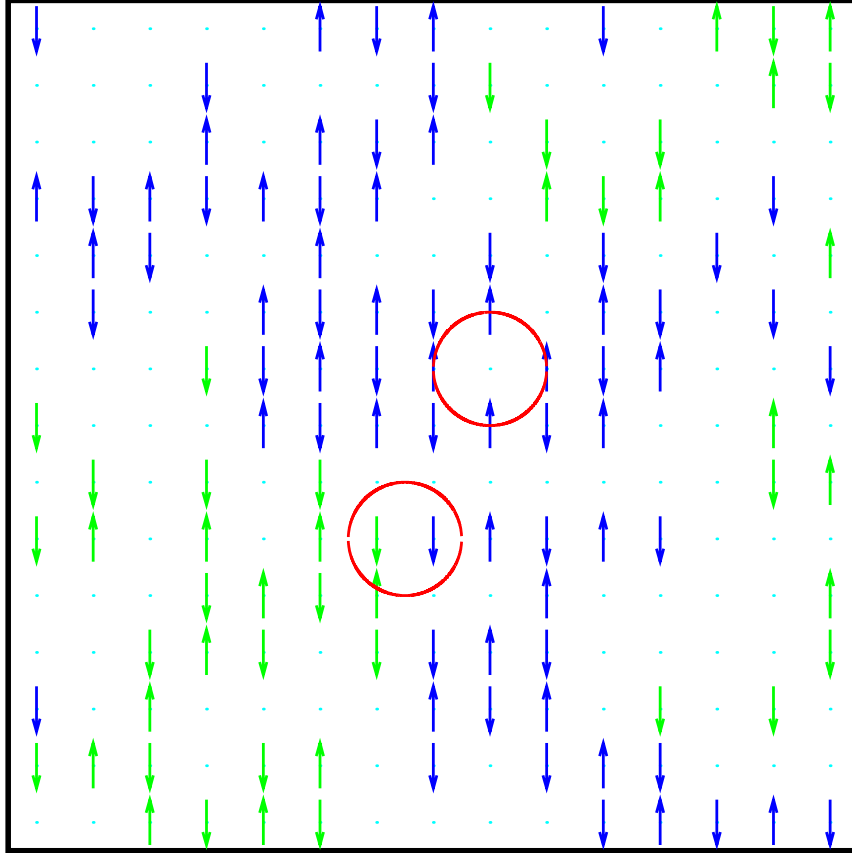


Figure 4: Snapshot of the same portion of the AFM interface monolayer after reversal of the FM ($B = -0.25J_{\text{INT}}$). The circles mark once again sources of magnetization where the domain wall magnetization is reversed while the volume magnetization is unchanged. The external field and the FM magnetization are now pointing down.

One contribution comes from parallel spin pairs in the domain walls, all pointing up in our example, i. e. into the direction of the exchange field of the FM and the external field. We will call this part in the following *domain wall magnetization*. A second contribution comes from an imbalance of the number of defects of the two antiferromagnetic sublattices. We will call this contribution in the following *volume magnetization*. The imbalance of the number of defects of the two antiferromagnetic sublattices also leads to a net magnetization within a domain which couples to the exchange field of the FM and the external field. The reason for the imbalance is that the domain structure is not random. Rather, it is an optimized structure arising during the initial cooling procedure with as much magnetization as possible coupling to the exchange field of the FM and the external field, following the energy minimization principle.

However, an AFM interface magnetization alone cannot lead to EB. Only the irreversible part of it (during hysteresis) may lead to EB. Figure 4 shows for comparison spin configurations in the same portion of the interface monolayer of the AFM after

reversal of the FM. Clearly, the bigger parts of the domain structure did not change during reversal of the FM. However, there are rearrangements on smaller length scales, leading mainly to the fact that the domain wall magnetization changes its sign. In Figure 4 all of the spin pairs within domain walls are pointing down following the reversed FM and the external field.

However, the volume magnetization coming from the defects remains frozen. The stability of the domain structure stems from the fact that the domain walls are pinned at defects sites as well as between pairs of spins which are aligned with the field. Hence, during a movement of the domain wall energy barriers may have to be overcome by thermal activation. This explains why a large domain in general will stay in a metastable state on exponentially long time scales, while rearrangements on a shorter length scale are possible, of course depending on the temperature and the material parameters of the AFM.

Many of the essential properties of diluted AFMs, the occurrence of domain states, metastability, remanent magnetization and slow relaxation, among others, have been investigated before, even though not in the context of EB (for reviews on diluted AFMs see [29, 30], for a detailed discussion of the connection between diluted AFMs and EB systems see [18]).

An important property of diluted AFMs is the slow relaxation of the remanent magnetization, i. e., the magnetization obtained after switching off the cooling field. Here it is known that the remanent magnetization of the DS relaxes non-exponentially on extremely long time scales after the field is switched off [31, 32, 33] or even within the applied field [34, 35, 36]. In the DS model EB is related to this remanent magnetization. This implies a decrease of EB due to slow relaxation of the AFM DS. Especially, the reason for the so-called training effect can be understood from Figs. 2, where it is shown that the hysteresis loop of the AFM interface layer is not closed on the right hand side. This implies that the DS magnetization is lost partly during the hysteresis loop due to a rearrangement of the AFM domain structure. This loss of magnetization clearly leads to a reduction of the EB for the next loop.

CONCLUSIONS

It was shown both, experimentally [15, 19] and by Monte Carlo simulations [15, 18], that diluting the AFM in the volume part away from the FM/AFM interface significantly enhances EB. This dilution supports the formation of domains in the volume of the AFM which carry magnetization. The DS of the AFM is to some extent frozen during hysteresis and this irreversible part of the DS magnetization at the AFM interface leads to EB.

In the domain state model, domain formation is crucial for the existence of EB. Without domain formation there would be no EB for compensated and a much too high EB for uncompensated interfaces. Defects in the AFM favor domain formation and thus make the distinction between compensated and uncompensated interfaces to a large extent obsolete. Also, it should be noted that the occurrence of a DS with an irreversible surplus magnetization is not restricted to diluted AFMs. Spin glasses, for instance, show similar features and it is known that the EB effect occurs also in compounds of FM and spin glass [3]. In these systems we believe the same mechanism leading to EB in our DS model is also

at work.

Important features of EB systems found experimentally [19] have their counterpart in the simulations [18], such as the order of magnitude of EB fields, the shape of hysteresis curves, the dilution dependence of EB, its temperature dependence, the training effect, and the occurrence of positive EB. The dependence of EB on thickness of the AFM is further discussed in [16], the dependence on the anisotropy of the AFM in [17].

Recent experiments [22, 23] which showed that EB can be modified by means of ion irradiating, i. e., by inducing defects in the bulk of the AFM underline the importance of defects for the understanding of EB. The DS model for EB in which the ion irradiation is modeled as a second dilution of the AFM after the initial cooling procedure explains the experimental facts in terms of domain rearrangements caused by diluting the system within an applied field [20].

In conclusion, our simulations strongly suggest that the existence of a DS in the AFM enhanced by defects or any other mechanism reducing the energy necessary to form domains in the volume part of the AFM, is a common feature of FM/AFM compounds showing a significant EB.

ACKNOWLEDGMENT

This work has been supported by the Deutsche Forschungsgemeinschaft through SFB 491. The authors thank B. Beschoten and G. Güntherodt for a fruitful cooperation.

References

- [1] W. H. Meiklejohn and C. P. Bean, *Phys. Rev.* **102**, 1413 (1956).
- [2] W. H. Meiklejohn and C. P. Bean, *Phys. Rev.* **105**, 904 (1957).
- [3] J. Nogués and I. K. Schuller, *J. Magn. Magn. Mat.* **192**, 203 (1999).
- [4] A. P. Malozemoff, *Phys. Rev. B* **35**, 3679 (1987).
- [5] A. P. Malozemoff, *J. Appl. Phys.* **63**, 3874 (1988).
- [6] A. P. Malozemoff, *Phys. Rev. B* **37**, 7673 (1988).
- [7] N. C. Koon, *Phys. Rev. Lett.* **78**, 4865 (1998).
- [8] D. Mauri, H. C. Siegmann, P. S. Bagus, and E. Kay, *J. Appl. Phys.* **62**, 3047 (1987).
- [9] T. C. Schulthess and W. H. Butler, *Phys. Rev. Lett.* **81**, 4516 (1998).
- [10] T. C. Schulthess and W. H. Butler, *J. Appl. Phys.* **85**, 5510 (1999).
- [11] M. D. Stiles and R. D. McMichael, *Phys. Rev. B* **59**, 3722 (1999).
- [12] M. Kiwi, J. Mejía-López, R. D. Portugal, and R. Ramírez, *Europhys. Lett.* **48**, 573 (1997).

- [13] K. Takano, R. H. Kodama, A. E. Berkowitz, W. Cao, and G. Thomas, *Phys. Rev. Lett.* **79**, 1130 (1997).
- [14] K. Takano, R. H. Kodama, A. E. Berkowitz, W. Cao, and G. Thomas, *J. Appl. Phys.* **83**, 6888 (1998).
- [15] P. Miltényi, M. Gierlings, J. Keller, B. Beschoten, G. Güntherodt, U. Nowak, and K. D. Usadel, *Phys. Rev. Lett.* **84**, 4224 (2000).
- [16] U. Nowak, A. Misra, and K. D. Usadel, *J. Appl. Phys.* **89**, 7269 (2001).
- [17] U. Nowak, A. Misra, and K. D. Usadel, *J. Magn. Magn. Mat.* **240**, 243 (2002).
- [18] U. Nowak, K. D. Usadel, P. Miltényi, J. Keller, B. Beschoten, and G. Güntherodt, *Phys. Rev. B* **66**, 14430 (2002).
- [19] J. Keller, P. Miltényi, B. Beschoten, G. Güntherodt, U. Nowak, and K. D. Usadel, *Phys. Rev. B* **66**, 14431 (2002).
- [20] A. Misra, U. Nowak, and K. D. Usadel, *J. Appl. Phys.* in press (2003).
- [21] H. T. Shi, D. Lederman, and E. E. C. Fullerton, *J. Appl. Phys.* **91**, 7763 (2002).
- [22] T. Mewes, R. Lopusnik, J. Fassbender, B. Hillebrands, M. Jung, D. Engel, A. Ehresmann, and H. Schmoranzer, *Appl. Phys. Lett.* **76**, 1057 (2000).
- [23] A. Mougin, T. Mewes, M. Jung, D. Engel, A. Ehresmann, H. Schmoranzer, J. Fassbender, and B. Hillebrands, *Phys. Rev. B* **63**, 60409 (2001).
- [24] F. Nolting, A. Scholl, J. Stöhr, J. W. Seo, J. Fompeyrine, H. Siegwart, J.-P. Locquet, S. Anders, J. Lüning, E. E. Fullerton, M. F. Toney, M. R. Scheinfein, and H. A. Padmore, *Nature* **405**, 767 (2000).
- [25] H. Ohldag, A. Scholl, F. Nolting, S. Anders, F. U. Hillebrecht, and J. Stöhr, *Phys. Rev. Lett.* **86**, 2878 (2001).
- [26] K. Binder and D. W. Heermann, in *Monte Carlo Simulation in Statistical Physics*, edited by P. Fulde (Springer-Verlag, Berlin, 1997).
- [27] U. Nowak, in *Annual Reviews of Computational Physics IX*, edited by D. Stauffer (World Scientific, Singapore, 2001), p. 105.
- [28] J. Nogués, C. Leighton, and I. K. Schuller, *Phys. Rev. B* **61**, 1315 (2000).
- [29] W. Kleemann, *Int. J. Mod. Phys. B* **7**, 2469 (1993).
- [30] D. P. Belanger, in *Spin Glasses and Random Fields*, edited by A. P. Young (World Scientific, Singapore, 1998).
- [31] S.-J. Han, D. P. Belanger, W. Kleemann, and U. Nowak, *Phys. Rev. B* **45**, 9728 (1992).

- [32] U. Nowak, J. Esser, and K. D. Usadel, *Physica A* **232**, 40 (1996).
- [33] M. Staats, U. Nowak, and K. D. Usadel, *Phase Transitions* **65**, 159 (1998).
- [34] J. Villain, *Phys. Rev. Lett.* **52**, 1543 (1984).
- [35] P. Pollak, W. Kleemann, and D. P. Belanger, *Phys. Rev. B* **38**, 4773 (1988).
- [36] U. Nowak and K. D. Usadel, *Phys. Rev. B* **39**, 2516 (1989).